

EFFECTS OF SIDE-WALL GROOVES ON TRANSMISSION CHARACTERISTICS OF SUSPENDED STRIP LINES

Eikichi Yamashita, Bai Yi Wang, and Kazuhiko Atsuki

University of Electro-Communications
Chofu-shi, Tokyo, Japan 182

ABSTRACT

The use of suspended strip lines is becoming a powerful transmission technique at millimeter wavelengths because of low attenuation, weak dispersion, and various merits in manufacturing processes. This paper estimates effects of side-wall grooves of these lines on transmission characteristics within the TEM wave approximation.

INTRODUCTION

Suspended strip lines (SSL's) were once used at low microwave frequencies as an application of early printed-circuit techniques before the appearance of microstrip lines. As introduced in the workshop on SSL filters in the 1984 International Microwave Symposium, SSL's have recently become very useful for millimeter wave transmission because of low attenuation, weak dispersion, moderate wavelength reduction factor, and various merits in manufacturing processes.

The transmission characteristics of SSL's as shown in Fig.1 were already analyzed both for thin-strip cases(1) and thick-strip cases(2). However, effects of side-wall grooves, which have been recently employed in practical SSL's to support substrates mechanically as shown in Fig.2, have not been estimated theoretically.

This paper shows the method and results of the quantitative analysis of such effects, particularly on the characteristic impedance and wavelength reduction factor.

METHOD OF ANALYSIS

The present analysis of transmission characteristics of SSL's with side-wall grooves is carried out within the TEM wave approximation since the weak dispersion of the dominant mode is expected because of the existence of two air regions. The past methods(1)(2) can not be applied to this structure because of its irregular shape.

The solution of Laplace's equation is first assumed for each of three regions. The strip conductor is assumed to be infinitely thin. Potential functions which satisfy boundary conditions at the surrounding conductor surface can be written in the form of Fourier series as

$$\phi_1(x,y) = \sum_{n=1,3,5}^{\infty} A_n \sinh\left(\frac{n\pi y}{a}\right) \cos\left(\frac{n\pi x}{a}\right) \quad (1)$$

$$\phi_2(x,y) = \sum_{n=1,3,5}^{\infty} [B_n \sinh\left(\frac{n\pi y}{a+2d}\right) + C_n \cosh\left(\frac{n\pi y}{a+2d}\right)] \cos\left(\frac{n\pi x}{a+2d}\right) \quad (2)$$

$$\phi_3(x,y) = \sum_{n=1,3,5}^{\infty} D_n \sinh\left[\frac{n\pi(b-y)}{a}\right] \cos\left(\frac{n\pi x}{a}\right) \quad (3)$$

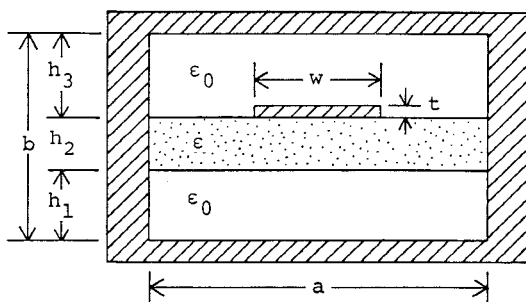


Fig. 1 Suspended Strip Lines (SSL).

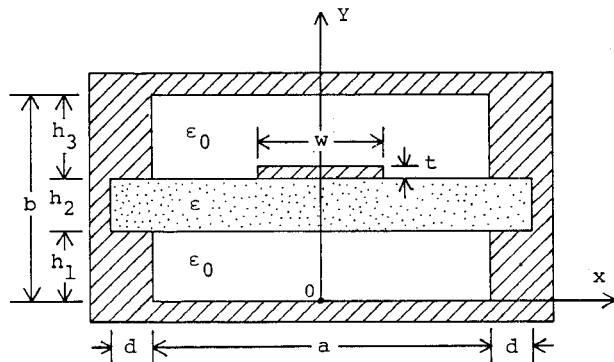


Fig. 2 Suspended Strip Lines with Side-Wall Grooves.

When potential functions at $y=h_1-0$, $y=h_1+0$, $y=h_1+h_2-0$, and $y=h_1+h_2+0$, are given by $f_1(x)$, $f_2(x)$, $f_3(x)$, and $f_4(x)$, respectively, the expressions, (1), (2), and (3), lead to the Fourier series expansions of these functions. The Fourier coefficients, A_n , B_n , C_n , and D_n are uniquely determined after knowing these functions. The variational method is useful to determine the form of these functions.

We now use the fact that the total electric field energy W of this structure per unit length is given by

$$W = \frac{1}{2} \sum_{i=1}^3 \epsilon_i \iint_{S_i} \left[\left(\frac{\partial \phi_i}{\partial x} \right)^2 + \left(\frac{\partial \phi_i}{\partial y} \right)^2 \right] dx dy \quad (4)$$

where S_i ($i=1,2,3$) denotes the cross-sectional area and ϵ_i ($i=1,2,3$) the dielectric constant of the region i . This energy can be minimized by changing the form of the above potential functions at $y = h_1$ and $y = h_1 + h_2$ as trial functions. The minimized energy W_{\min} is related to the line capacitance C by

$$W_{\min} = \frac{1}{2} C V^2 \quad (5)$$

where V denotes the potential difference between the strip and wall conductor. Then, the characteristic impedance Z and the wavelength reduction factor λ/λ_0 within the TEM wave approximation are given by

$$Z = \frac{1}{v_0 \sqrt{C C_0}} \quad (6)$$

$$\frac{\lambda}{\lambda_0} = \sqrt{\frac{C_0}{C}} \quad (7)$$

where v_0 is the velocity of light in vacuum and C_0 is the line capacitance for the case $\epsilon_1 = \epsilon_2 = \epsilon_3 = \epsilon_0$.

TRIAL FUNCTIONS

Because of the symmetry of the structure, the potential functions have also even symmetry and only a half of the structure has to be treated. The above four functions in the right half are mutually related as

$$f_1(x) = f_2(x) = f(x) \quad (0 \leq x \leq \frac{a}{2}) \quad (8)$$

$$f_2(x) = 0 \quad (\frac{a}{2} \leq x \leq \frac{a}{2} + d) \quad (9)$$

$$f_3(x) = f_4(x) = g(x) \quad (\frac{w}{2} \leq x \leq \frac{a}{2}) \quad (10)$$

$$f_4(x) = 0 \quad (\frac{a}{2} \leq x \leq \frac{a}{2} + d) \quad (11)$$

We choose the first-order spline function (or the polygonal line function) as trial functions to express $f(x)$ and $g(x)$ as shown in Fig. 3, because

the spline function has a simple form and is useful in approximating complicated curves.

The values of potential functions at the knots of the spline function are denoted by $p_0, p_1, p_2, \dots, p_{m1}$, for $f(x)$, and q_1, q_2, \dots, q_{m2} for $g(x)$. These potentials are new variables and used to minimize the electric field energy W by conditions as

$$\frac{\partial W}{\partial p_i} = 0 \quad (i = 0, 1, 2, \dots, m_1 - 1) \quad (12)$$

$$\frac{\partial W}{\partial q_j} = 0 \quad (j = 1, 2, 3, \dots, m_2 - 1) \quad (13)$$

By imposing these conditions on the trial functions, we obtain a set of linear, simultaneous, inhomogeneous equations which can be solved on a computer. As a result, explicit potential functions are found in the whole region.

NUMERICAL RESULTS

The length of computation time is closely related to the number of knots, m_1 and m_2 , and can be minimized by taking the following measures:

- 1) The size of m_1 and m_2 are increased when those of a/b and $(a-w)/2b$ are increased, respectively.
- 2) The knots of the spline function for $g(x)$ near the strip conductor are narrowly spaced to represent potential curves precisely.

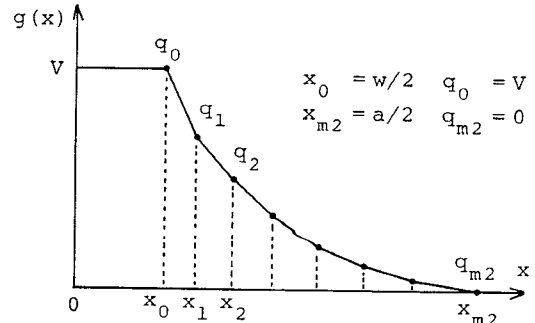
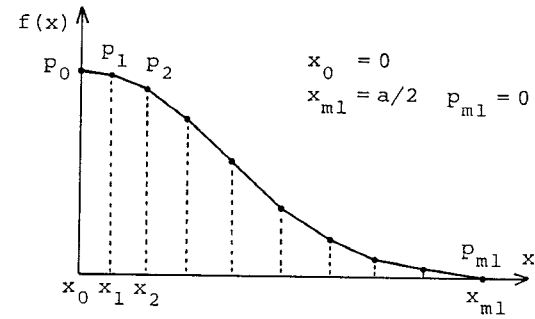


Fig. 3 Trial Functions in the Form of Spline Function.

Since the common values of the characteristic impedance are 50Ω and 75Ω , structural dimensions of SSL's in this paper are also selected by considering these values. Relatively high walls are treated in order to see strong effects of side-wall grooves on the characteristic impedance. For Duroid ($\epsilon^* = 2.22$) used as substrates, the following sets of dimensions are treated:

$$\begin{aligned} a/b &= 1.0 \\ h_1/b = h_3/b &= 0.4 \\ h_2/b &= 0.2 \\ t/b &= 0 \\ w/b &= 0.2 \sim 0.9 \\ d/b &= 0 \sim 0.5 \end{aligned}$$

Fig.4 shows the convergence of the characteristic impedance for the increase of the total number of knots, $m = m_1 + m_2$.

Typical results of numerical calculations are shown in Fig.5 and 6. In this case, the number of truncated series terms $N=100$, $m_1=7$, and $m_2=13$. It is seen that when the deeper grooves are made the higher impedance and higher wavelength reduction factor are obtained. These effects can not be neglected when precise filters are designed. In order to avoid these effects very low side-walls ($b \ll a$) must be employed. It should be noted that the size of the width a also affects the lowest cutoff frequency.

This method of analysis is simple and efficient for numerical computation. The time required for obtaining a set of the characteristic impedance and the wavelength reduction factor was about 8 sec. on a HITAC-M180 computer.

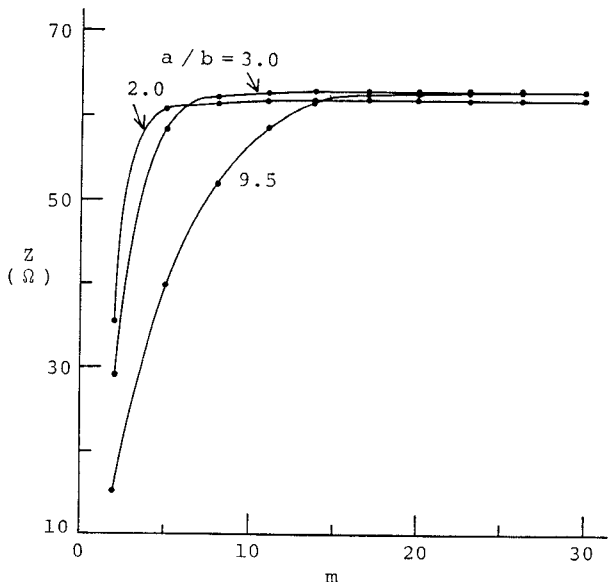


Fig. 4 The Convergence of the Impedance Value for Increasing the Number of Knots, m .
 $w/b = 1.0$ $h_1/b = h_3/b = 0.4$ $h_2/b = 0.2$
 $d/b = t/b = 0$ $\epsilon_1^* = \epsilon_2^* = \epsilon_3^* = 1.0$

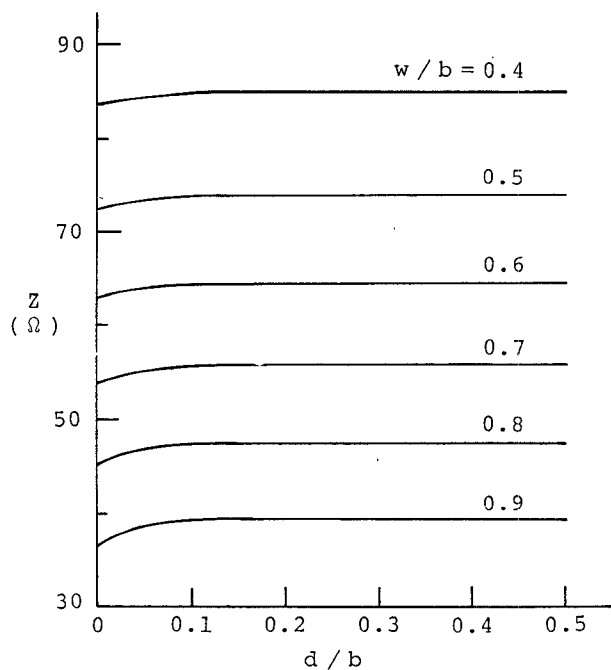


Fig. 5 Effects of Side-Wall Grooves on the Characteristic Impedance.

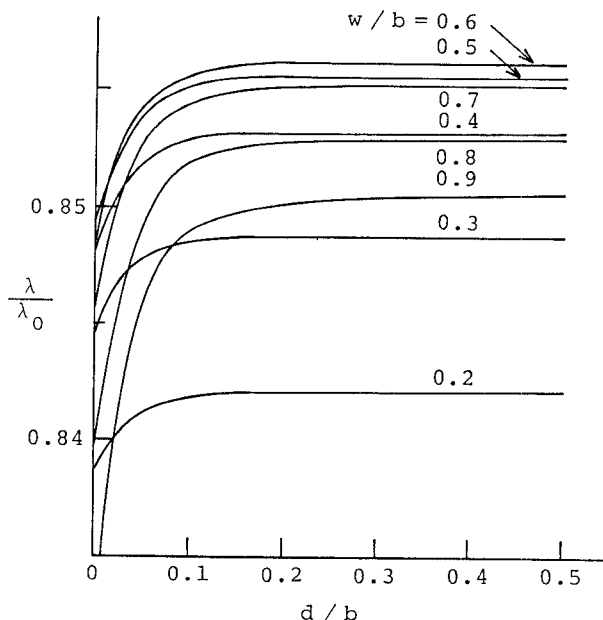


Fig. 6 Effects of Side-Wall Grooves on the Wavelength Reduction Factor.

Fig. 7 shows some of possible structures to which this analysis method can be applied.

ACKNOWLEDGEMENT

The authors thank Dr. Y.Suzuki for his helpful comments and Graduate Student K.R.Li for his assistance.

REFERENCES

- (1) E.Yamashita and K.Atsuki, "Strip lines with rectangular outer conductor and three dielectric layers," IEEE Trans. MTT, vol. MTT-18, pp. 238-242, May 1970.
- (2) K.Atsuki and E.Yamashita, "Analytical method for transmission lines with thick-strip conductor, multi-dielectric layers, and shielding conductor," IECE of Japan, vol.53-B, pp. 322-328, June 1970.

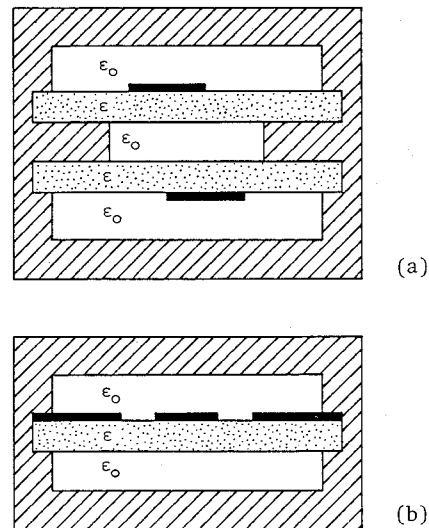


Fig. 7 (a) Coupled SSL's. (b) Coplanar SSL's.